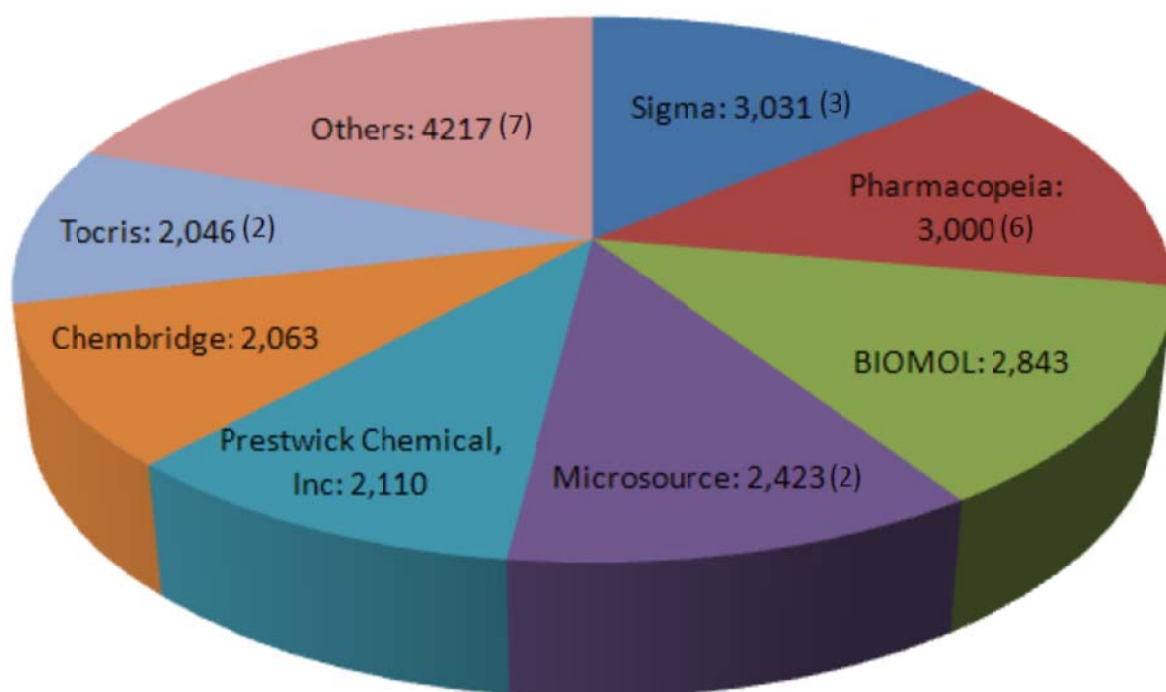
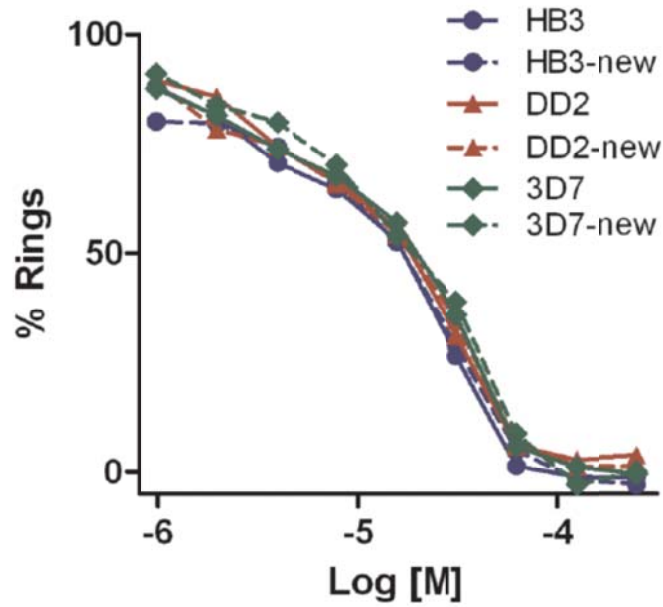


**Supplementary Figure S1. Optimization of the miniaturized high-throughput AlphaScreen**

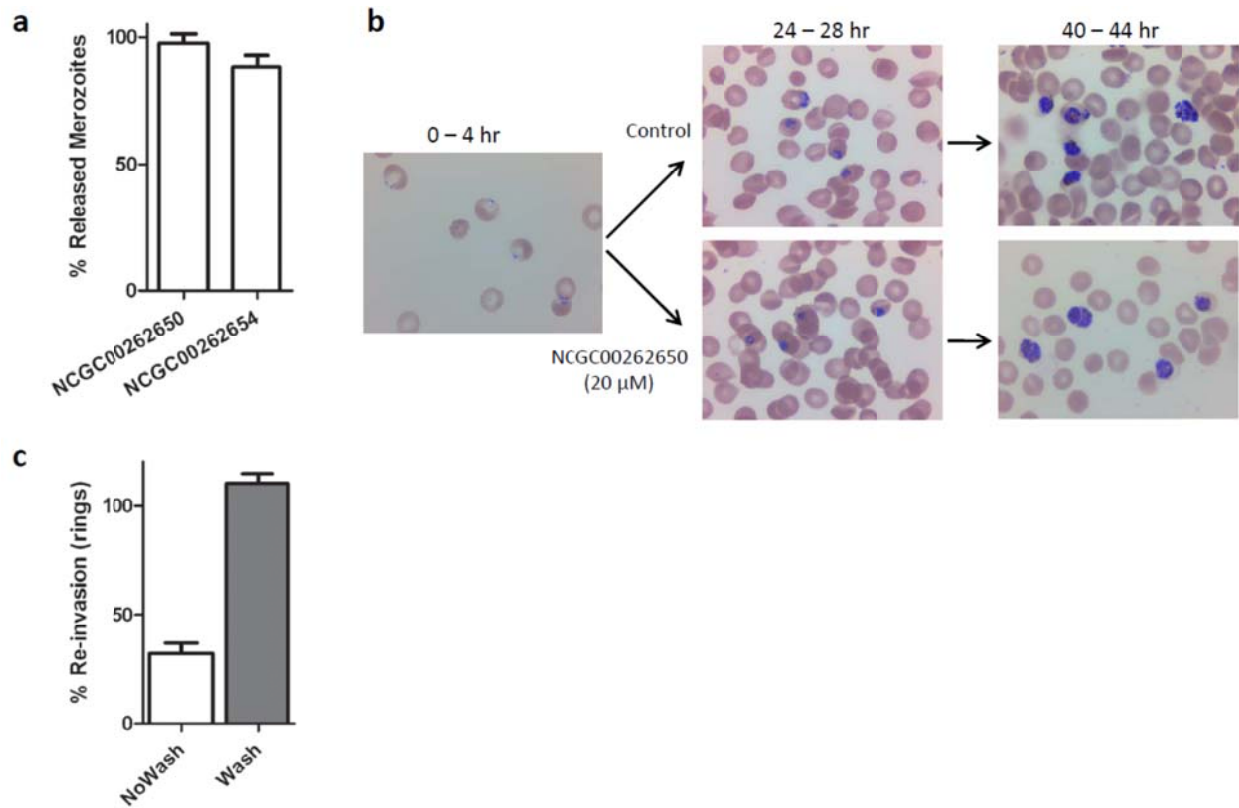
**assay.** (a) Titration of RON2L peptide–AMA1(3D7) protein binding matrices in 1,536-well format. Subsequently, 25 nM each of the RON2L peptide and AMA1(3D7) protein were chosen for the HTS based on the optimal signal to noise ratio. Error bars represent  $\pm$  SEM from 3 independent experiments. (b) The relatively constant hashed bars over time indicate good reagent stability and excellent assay statistical performance ( $\bullet$ ; Z' factor). (c) Consistent statistical (O; Z' factor) performance and stable  $IC_{50}$  values obtained using the positive control R1 peptide inhibitor ( $\blacksquare$ ).



**Supplementary Figure S2. Libraries used in the high throughput AlphaScreen.** The pie chart illustrates the sources of the compounds and the number of compounds from each source used in the AlphaScreen assay. Numbers within parenthesis indicates the number of compounds within the library that were confirmed to inhibit the binding of AMA1 and RON2.



**Supplementary Figure S3. Activity of re-synthesized NCGC0015280 is comparable to the commercially available compound.** Purified schizonts from three genetically different parasites were allowed to rupture and invade new RBCs for 4 hr in the presence of varying concentrations of the re-synthesized (new and commercially available compound (Sigma)). Error bars represent  $\pm$  SEM from 2 independent experiments for each parasite clone. The number of parasites in the absence of inhibitor was considered 100%.

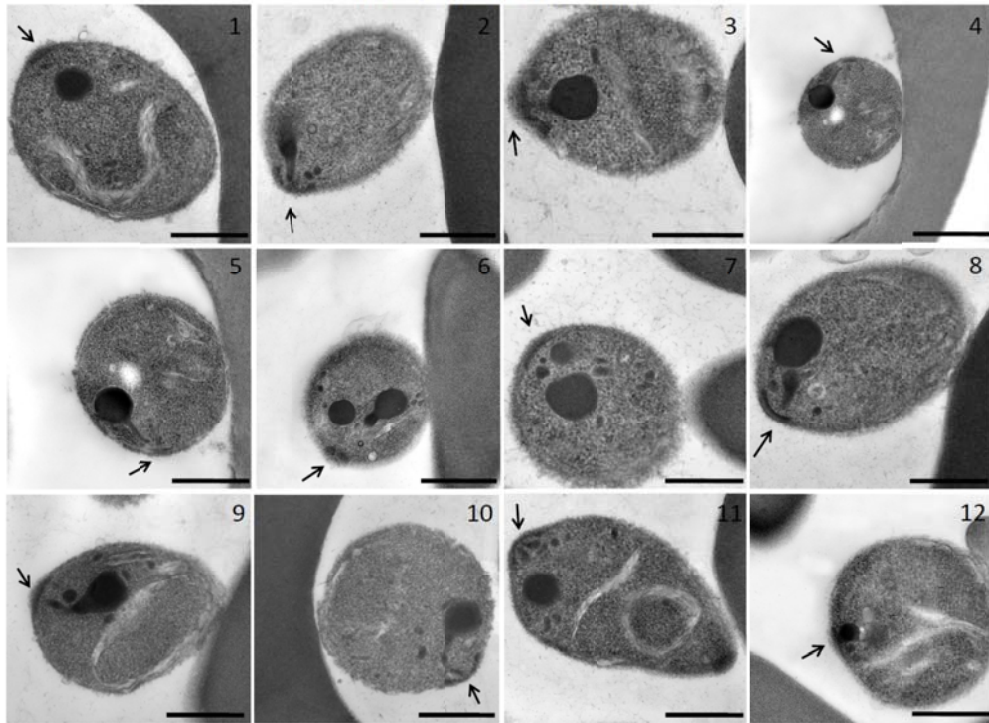


**Supplementary Figure S4.** Intracellular development is not significantly affected. (a) Merozoite release from schizont-infected RBCs is not affected by inhibitors. The number of merozoites released in the presence of 6  $\mu$ M (NCGC00262650) and 12  $\mu$ M (NCGC00262654) inhibitors, the  $IC_{50}$  for merozoite invasion, was counted on a hemocytometer. Error bars represent  $\pm$  SEM from two experiments for each compound. The number of parasites in the absence of inhibitor was considered 100%. (b) Intracellular parasite development is not affected. Early ring stage parasites (0 – 4 hr after invasion) were allowed to develop in the absence (control) or presence of 20  $\mu$ M NCGC00262650 and Geimsa stained after 24 and 40 hr to monitor parasite development. (c) Merozoite maturation is not affected. Ring stage parasites grown in the presence of NCGC00262650 (20  $\mu$ M) was washed after 40 hr and resuspended in complete media with (NoWash) or without (Wash) 10  $\mu$ M NCGC00262650 and assayed for merozoite re-

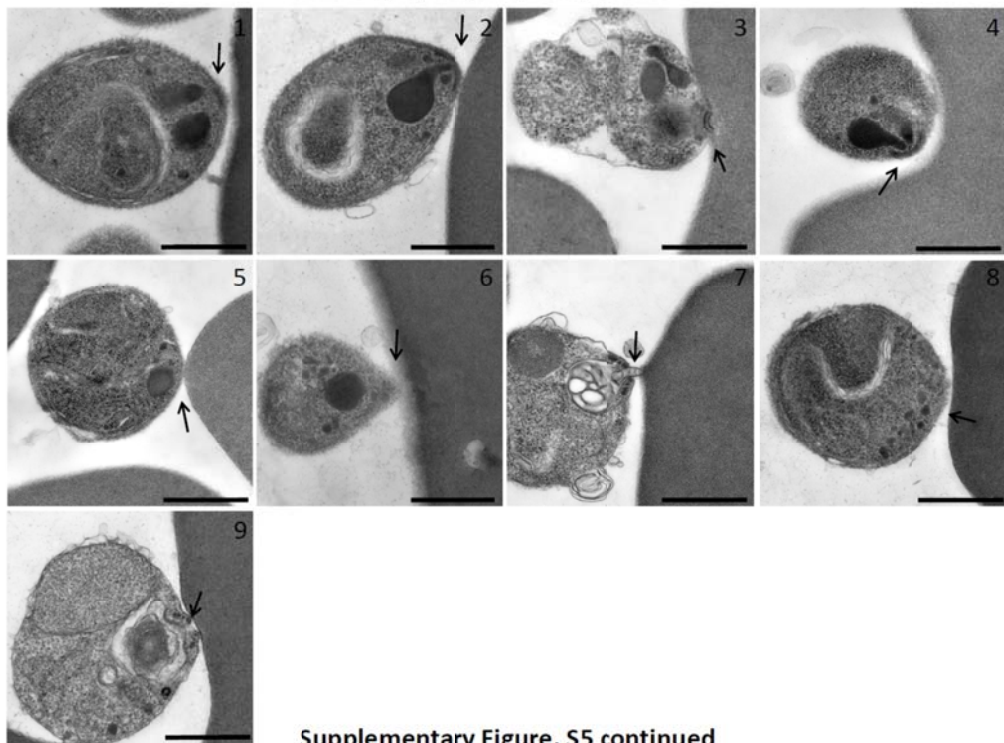
invasion (6 – 8 hr). Control parasites grown in the absence of inhibitor was used as 100%.

Experiment was performed in triplicate and error bars represent  $\pm$  SEM.

Control (+CytoD) : Not Apical



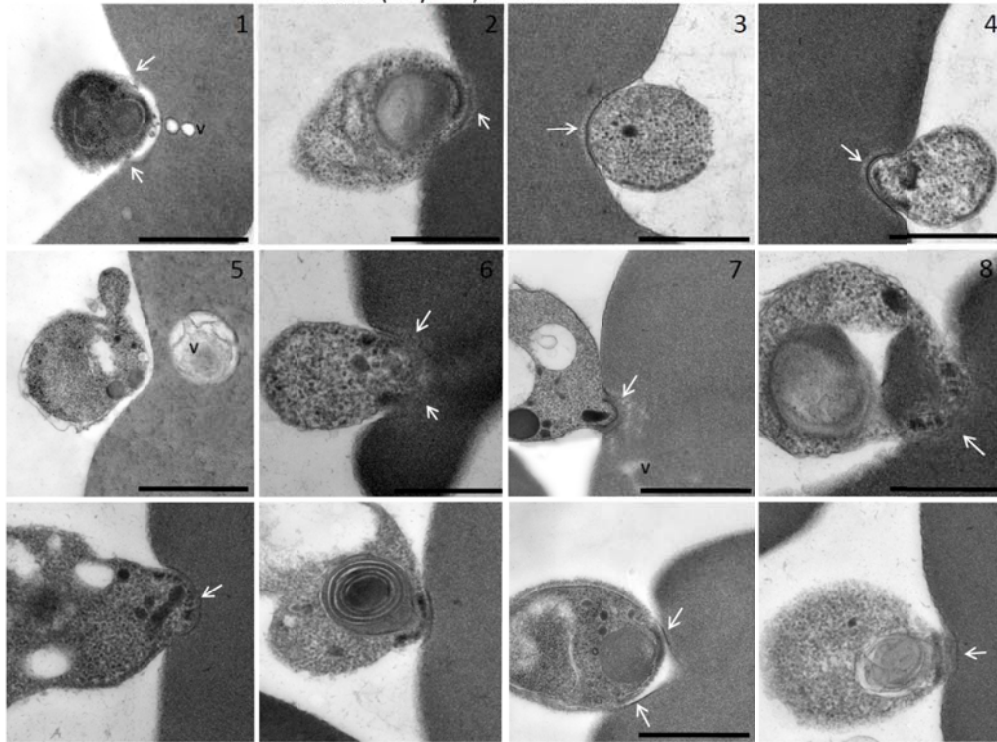
Control (+CytoD) : Apically oriented



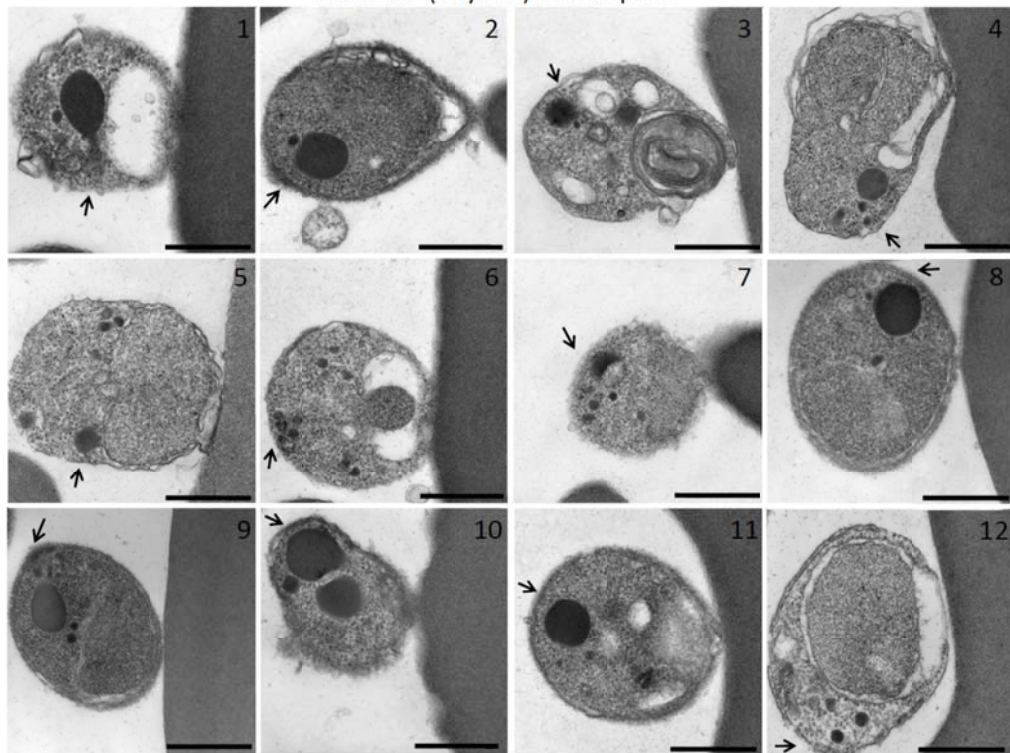
Supplementary Figure. S5 continued



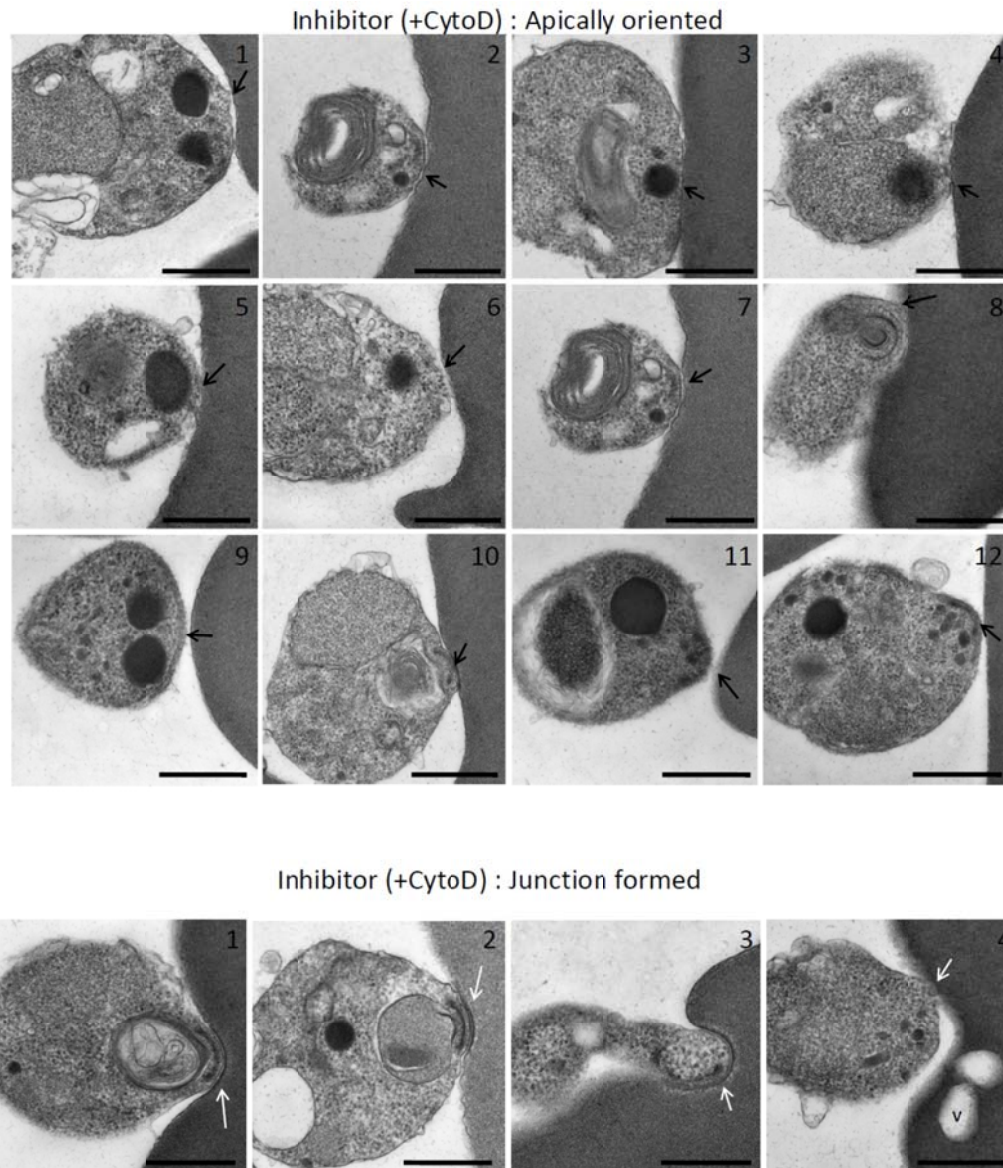
Control (+CytoD) : Junction formed



Inhibitor (+CytoD) : Not Apical

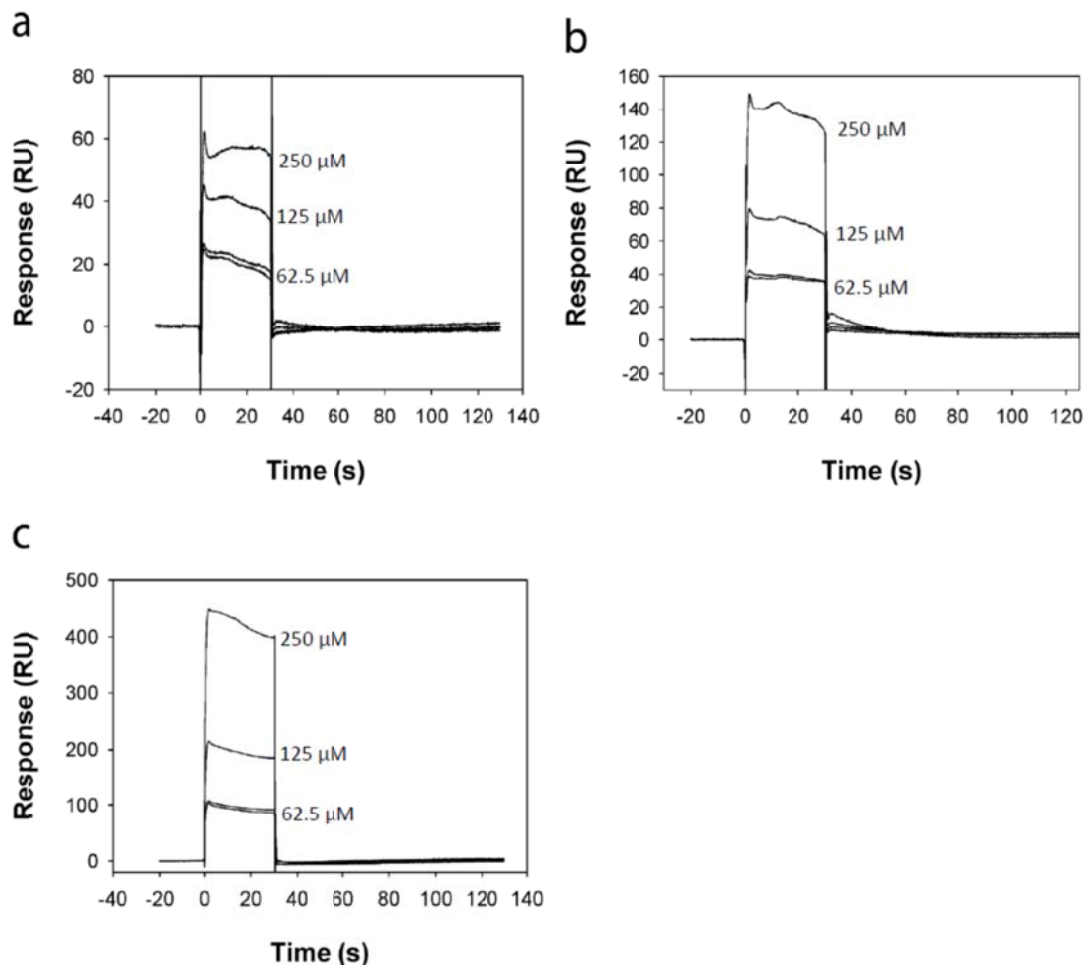


Supplementary Figure. S5 continued

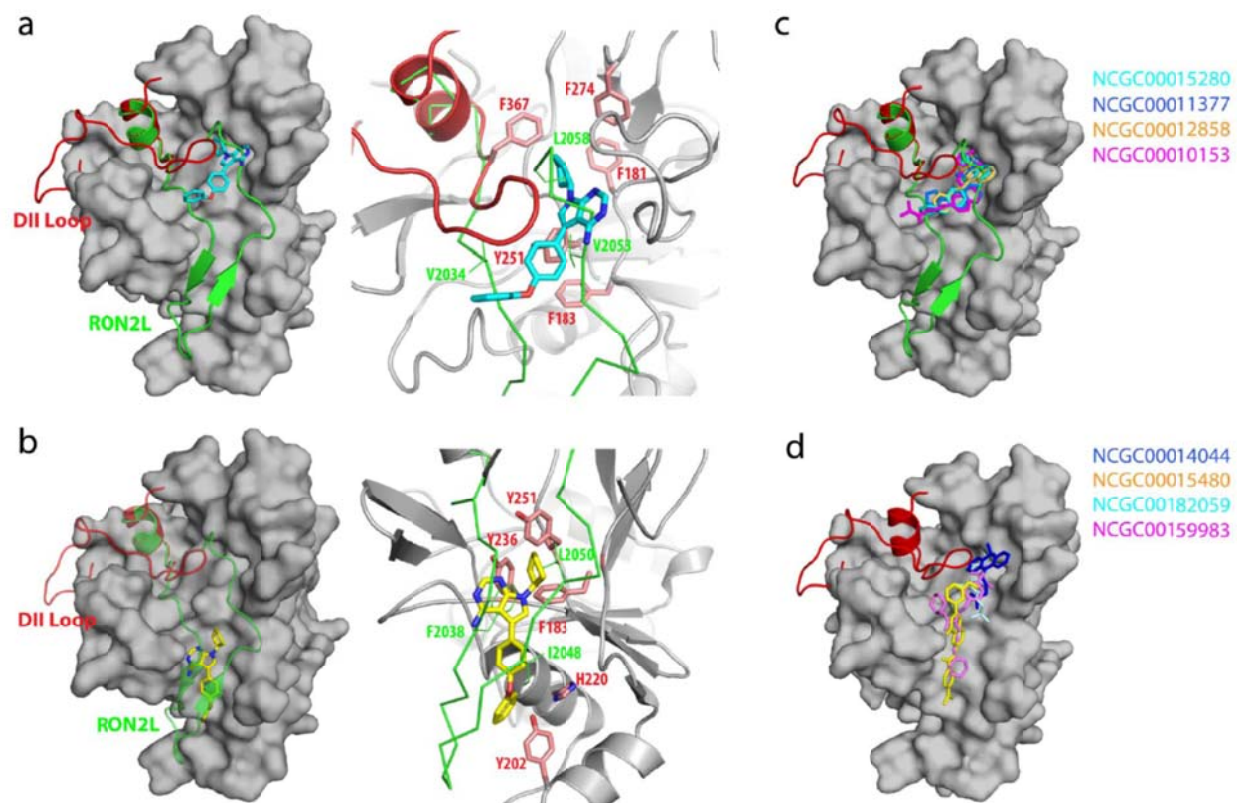


**Supplementary Figure S5.** AMA1-RON2 inhibitors block junction formation. Parasites (not apical, apically reoriented and junction formed merozoites) that were used for quantitation in Fig.5b and 5c are shown. Black arrows point to the apical end of the merozoite , white arrows indicates junction formation. Scale bars represent 250 nm.

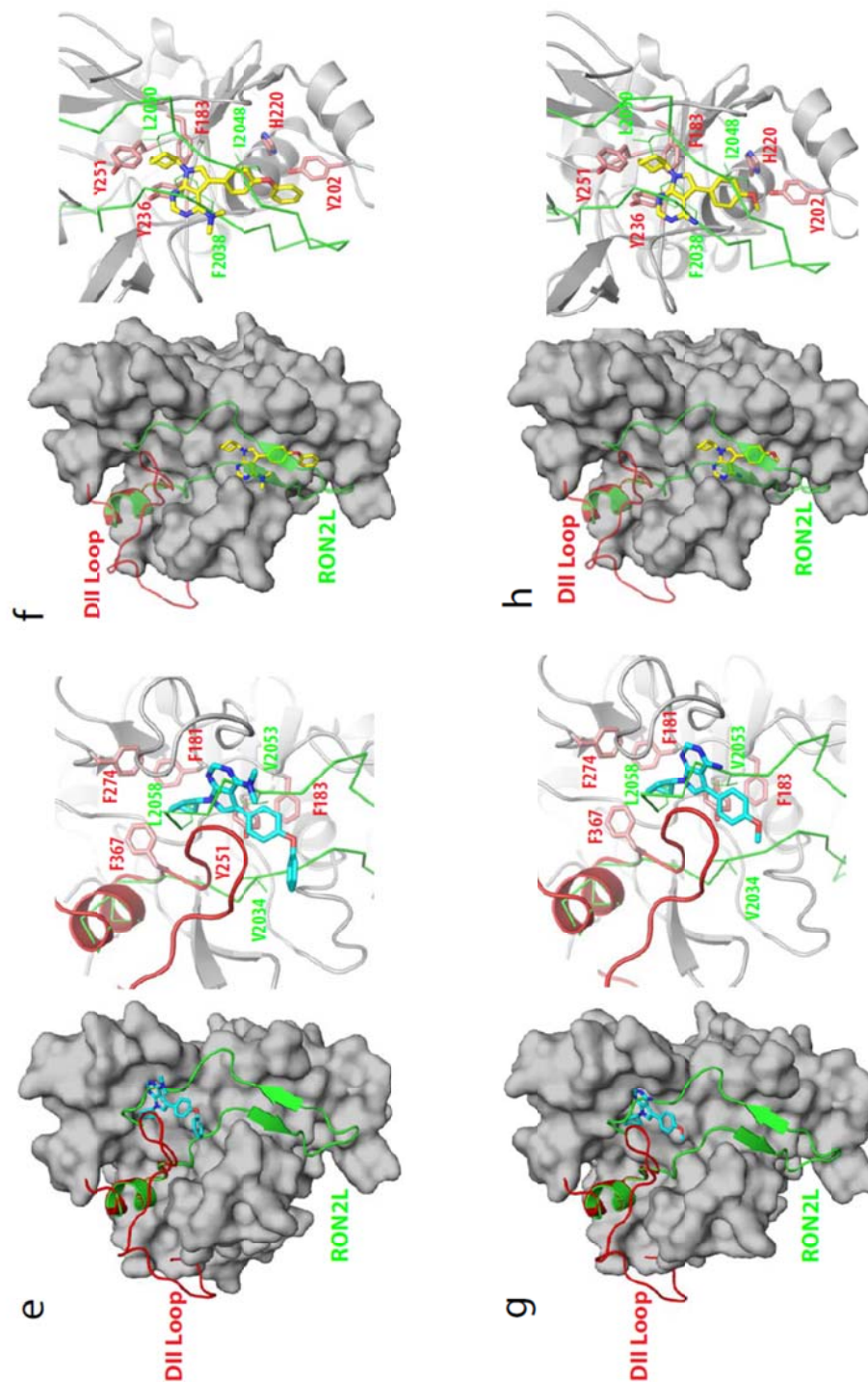




**Supplementary Figure S6.** Surface Plasmon Resonance (SPR) sensograms of different concentrations of the AMA1-RON2 inhibitors (250  $\mu$ M, 125  $\mu$ M and 62.5  $\mu$ M) binding to the 66 kd AMA1 ectodomain immobilized on a CM5 sensor chip. The inhibitors used are NCGC00015280 (a), NCGC00262650 (b) and NCGC00181034 (c). The data indicates that the inhibitors bind AMA1 confirming the direct binding demonstrated by the depletion assay. Kinetics could not be assessed accurately as the effective concentration of the inhibitors could not be determined due to poor solubility of the compounds in the SPR buffer.



Supplementary Figure. S7 continued



**Supplementary Figure S7.** *In silico* modeling of inhibitor binding to AMA1. (a) Binding model 1 of compound NCGC00015280 with AMA1. (b) Binding model 2 of compound NCGC00015280 with AMA1. (c) Binding model of compounds in cluster 1 with AMA1. (d) Binding model of

singletons with AMA1. The apo structure of AMA1 is illustrated in surface representation (grey) and domain II loop is shown as ribbons (red). The RON2 peptide is superimposed from the AMA1-RON2 complex and is shown as ribbons (green). Key residues in the hydrophobic pocket are shown as sticks. (e, f) Binding model 1 and 2 of analog NCGC00262654. (g,h) Binding model 1 and 2 of analog NCGC00262650.

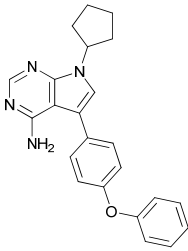
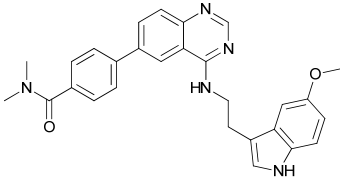
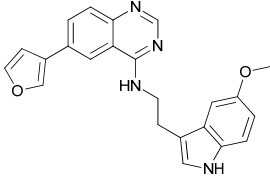
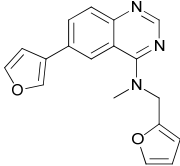
**Supplementary Table S1.** AlphaScreen IC<sub>50</sub> values of AMA1(3D7 allele)-RON2L inhibitors, IC<sub>50</sub> values of compounds active in the SYBR green assay against heterologous FVO parasite and % invasion at 25 µM and 50 µM using purified, invasive merozoite.

Sample ID	Sample Name	Alpha Screen	SYBR green Assay	Merozoite Invasion (%)	
		IC <sub>50</sub> (µM)	IC <sub>50</sub> (µM)-FVO	50 µM	25 µM
NCGC00015280	7-Cyclopentyl-5-(4-phenoxy)phenyl-7H-pyrrolo[2,3-d]pyrimidin-4-ylamine	21	28	20	47
NCGC00181034	Liarozole hydrochloride	29	29	54	64
NCGC00014044	Dimetacrine	28	30	23	56
NCGC00015589	3-[4-Iodophenyl]-1-piperazyl methylpyrrolo [2,3-b] pyrimidine	14	31	87	96
NCGC00011377		22	32	89	95
NCGC00012548		35	33	Not tested	Not tested
NCGC00024547	nor-Binaltorphimine	20	34	100	100
NCGC00015480	GW7647	27	Not active	Not tested	Not tested
NCGC00015672	Morin	15	Not active	Not tested	Not tested
NCGC00074700		15	Not active	Not tested	Not tested
NCGC00074720		25	Not active	Not tested	Not tested
NCGC00074725		18	Not active	Not tested	Not tested
NCGC00074728		23	Not active	Not tested	Not tested
NCGC00182059	Febuxostat	13	Not active	100	100
NCGC00010153		21	Not tested	Not tested	Not tested
NCGC00012125		26	Not tested	Not tested	Not tested
NCGC00012858		25	Not tested	Not tested	Not tested
NCGC00012896		25	Not tested	Not tested	Not tested
NCGC00025139		25	Not tested	Not tested	Not tested
NCGC00159983		26	Not tested	Not tested	Not tested

See methods for experimental details. The 3D7 allele of AMA1 was used in the AlphaScreen assay. SYBR green assay was performed using the *Pf* FVO clone that carries a heterologous allele of AMA1. Merozoite invasion assay was performed using the FVO clone selected for merozoites that retain invasiveness after purification.

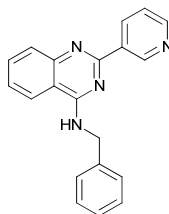


**Supplementary Table S2.** Structures of AlphaScreen actives. The structures of the AlphaScreen active compounds can be grouped into two major clusters. Cluster 1 contains six compounds that contain a benzopyrimidine or benzoimidazole-like functional core and an extended aromatic group. All tested compounds from cluster 1 (3/6) were active in the SYBR green assay. Hits in the second cluster are peptidic compounds containing multiple acidic and polar groups. All Cluster 2 compounds were inactive (5/5) in the SYBR green assay. The rest were singletons (9 compounds) of which five of the tested compounds (5/7) were active in the SYBR green assay.

Sample ID	NCGC ID	Cluster	Structure	SYBR green Assay	PubChem SID
NCGC00015280-05	NCGC00015280	1		Active	124879782
NCGC00010153-01	NCGC00010153	1		Not tested	4237624
NCGC00012896-01	NCGC00012896	1		Not tested	4240367
NCGC00011377-01	NCGC00011377	1		Active	4238848

NCGC00012858-01    NCGC00012858

1

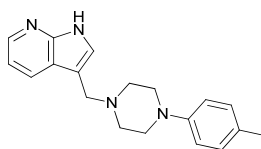


Not  
tested

4240329

NCGC00015589-03    NCGC00015589

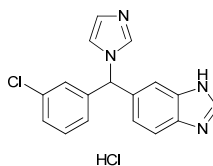
1



Active

124880514

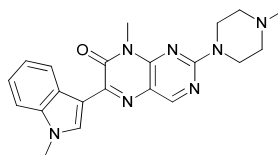
NCGC00181034-01    NCGC00181034    singleton



Active

144206236

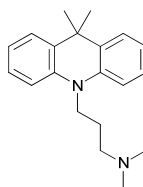
NCGC00012548-01    NCGC00012548    singleton



Active

4240019

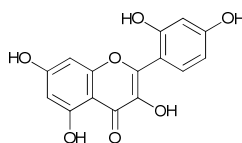
NCGC00014044-01    NCGC00014044    singleton



Active

144203594

NCGC00015672-14    NCGC00015672    singleton



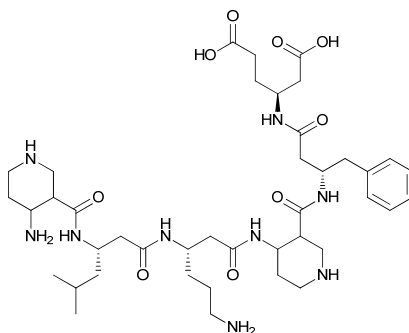
Active

90341521



NCGC00074700-01 NCGC00074700

2

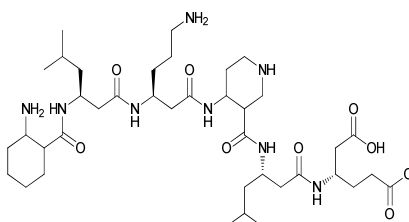


Inactive

11114346

NCGC00074720-01 NCGC00074720

2

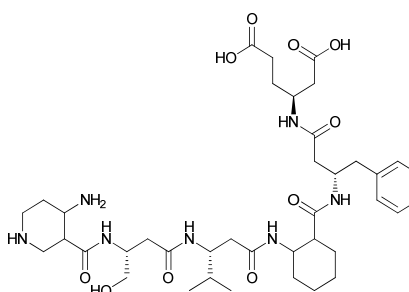


Inactive

11114366

NCGC00074725-01 NCGC00074725

2



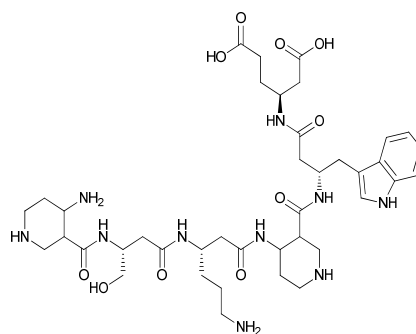
Inactive

11114371

NCGC00074728-01

NCGC00074728

2



Inactive

11114374



## SUPPLEMENTARY METHODS

### AMA1-RON2L AlphaScreen Assay

Briefly, 2  $\mu$ L of his-tagged AMA1 (3D7 allele) protein (final concentration 25 nM) was dispensed into a 1,536-well assay plate followed by 1  $\mu$ L of biotinylated RON2 peptide (final concentration 25 nM). Unlabeled RON2 peptide or R1 peptide (VFAEFLPLFSKFGSRMHILK) that specifically binds the 3D7 AMA1 was used as a positive control that inhibited the binding of RON2L to AMA1. Small molecules and positive control peptides were pin-transferred (23 nL or 46 nL) via Kalypsys pin-tool equipped with a 1536-pin array, resulting in final compound and peptide concentration ranges of 1.93 nM – 114  $\mu$ M, and 15.6 nM – 2.00  $\mu$ M, respectively. A total of 21,733 compounds were used in the primary screen (Fig. S2). The assay plate was then incubated for 30 minutes at RT (protected from light), followed by an addition of 1  $\mu$ L mixture of donor and acceptor beads (10  $\mu$ g/mL each final concentration). Samples were incubated for an additional 30 min at RT and read using an EnVision® Multilabel Reader (PerkinElmer).

A counterscreen assay was performed substituting a biotinylated-(His)<sub>6</sub> linker for the biotin-RON2L peptide and his-tagged AMA1 protein was used in the AlphaScreen assay. This assay was used to identify false positive compounds that disrupted the energy transfer from donor beads to acceptor beads (quenchers) or ones that non-specifically disrupted the binding between beads and the linker. Selected compounds were re-confirmed using the AlphaScreen assay. Validated compounds were analyzed *in silico* to remove compounds with poor development potential using three filters, namely, PAINS<sup>41</sup>, Lilly Medchem filters (<http://tripod.nih.gov/siphonify/>) and the NCGC filter collection (<http://pubs.acs.org/doi/full/10.1021/jm901070c>). Percent activity was derived using in-house software (<http://tripod.nih.gov/curvefit/>). Z' factor index, a measure of assay quality control, was

determined by  $Z' = 1 - (3 \times SD_{\text{neutral control}} + 3 \times SD_{\text{positive control}}) / (\text{Mean}_{\text{neutral control}} - \text{Mean}_{\text{positive control}})$  where SD is the standard deviation, , the neutral and positive control are the reaction with and without the biotinylated RON2 peptide, respectively.

### **High throughput SYBR green assay to measure RBC invasion**

Briefly, 4  $\mu\text{L}$  of culture medium was first dispensed into clear-bottom, 1536-well plates (Aurora Biotechnologies) using a Multidrop Combi dispenser (Thermo Fisher Scientific Inc.). Next, using a pin tool (Kalypsys) 23 nL of 3-fold serially diluted compounds in DMSO (0.29% final concentration) was added to each well in triplicate. Subsequently, 4  $\mu\text{L}$  of synchronized *P. falciparum* (FVO clone) schizonts were added to each well (2% parasitemia, 1% hematocrit final concentration) and incubated at 37°C in a humidified incubator in 5% CO<sub>2</sub> for 36 hr to allow merozoites release and invasion of RBCs and development to the trophozoite stage. At the this time, 2  $\mu\text{L}$  of lysis buffer (20 mM Tris-HCl, 10 mM EDTA, 0.16% saponin, 1.6% triton-X, 10X SYBR Green I (Invitrogen)) was added to each well and incubated for 4 hr. Fluorescence intensity at 485 nm excitation and 535 nm emission wavelengths was measured on an EnVision (Perkin Elmer) plate reader to evaluate the inhibitory activity of the compounds. Cytochalasin D (2  $\mu\text{M}$ ) that blocks merozoite invasion was used as a positive control as well as to estimate the background fluorescence in the absence of merozoite invasion. Each compound was tested in at least 3 independent experiments.

**SYBR Green Drug Assay.** Assays were performed as described previously <sup>42</sup> with some minor modifications. Briefly, synchronized schizont-infected RBCs (3D7 or FVO) were dispensed into 96-well plates containing the individual inhibitors or in combination (2% parasitemia , 1% hematocrit and inhibitors NCGC00015280 (8  $\mu\text{M}$ ), NCGC00262650 (8  $\mu\text{M}$ ) and DHA (3 nM) final concentration).

Parasites were allowed to develop for 36 hr at 37 °C after which DNA content was measured by staining with SYBR Green I as described. Parasite growth in the absence of inhibitor and wells containing no parasites were used as controls. Each assay was performed in duplicate. Signals were read in a FluoStar microplate reader (BMG Labtech, Germany). The mean growth inhibition under each condition was calculated using GraphPad Prism 5.0 software package (San Diego, CA) and statistical analysis was performed by one-way ANOVA and *P*-value significance calculated using Bonferroni's multiple comparison test.

### **Schizont rupture assay**

Purified, schizont-infected RBCs (FVO clone) were incubated at 37°C for 3 hr in the presence of the inhibitors at the indicated concentrations. The numbers of released merozoites were counted using a hemocytometer. The number of free merozoites in the absence of any inhibitors was considered 100%.

### **Co-immunoprecipitation and Western blotting**

Schizont-infected RBCs from synchronized *P. falciparum* FVO parasites were used for immunoprecipitation. Briefly,  $3 \times 10^6$  schizont-infected RBCs were lysed in the presence of 100 µM of each of the inhibitors in ice-cold parasite solubilization buffer (50mM Tris.HCl pH7.5, 150mM NaCl, 2mM EDTA, 1% Triton X-100, and protease inhibitor cocktail (Roche). Equal amount of PBS or DMSO was used as a negative control. RON2L peptide (50 µg, final concentration 55 µM) that inhibits AMA1- RON complex formation was used as positive control. After incubating on ice for 2 hr, samples were centrifuged at 15,000 RPM for 15 min and the supernatant was incubated with mouse anti-RON4 mAb (5 µg). After pulling down the complex using anti-mouse IgG, bound proteins were eluted in SDS loading buffer and run on 5-25% SDS-PAGE gels and transferred to a PVDF membrane. Blots were

probed first with rabbit anti-AMA1 antibody and detected using HRP-conjugated anti-rabbit antibody (Sigma). The same blots were re-probed using mouse anti-RON4 antibody and detected using conformation-specific HRP-conjugated anti-mouse antibody (eBioscience). Two independent experiments were performed.

### **Flow cytometry measurement of merozoite invasion**

Follow-up assays utilized flow cytometry measurements to evaluate the inhibitory activity of selected compounds. Invasion assays were carried out starting with either purified, schizont-infected RBCs or free, invasive merozoites. For assays using schizont-infected RBCs: fully mature parasites from the FVO, 3D7, DD2 and HB3 clones were purified on a 70-40 percol/sorbitol gradient and mixed with freshly prepared, pre-warmed RBCs. Merozoites were allowed to rupture and invade fresh RBCs (2 to 4% parasitemia, 1% hematocrit final) for 4 to 6 hr at 37°C in the presence of varying concentrations of the inhibitors as indicated. For assays using merozoites: Merozoites from a *P. falciparum* clone FVO, selected for prolonged survival was isolated as described previously<sup>19</sup>.  $\sim 5 \times 10^7$  merozoites were mixed with  $2.5 \times 10^7$  pre-warmed RBCs (500  $\mu$ L final volume) in the presence of varying concentrations of the inhibitors, gassed and incubated at 37°C for 3 to 4 hr. Free merozoites were removed from RBCs by centrifugation at 50 g for 7 min and the resulting RBC pellet contains newly invaded rings. For flow cytometry measurement,  $\sim 5 \times 10^7$  cells (infected and uninfected RBCs) were incubated with 1X SYBR green (Invitrogen) that labels DNA and mitotracker red (Invitrogen) that stains viable mitochondria for 30 min at room temperature (final volume 40  $\mu$ L). Stained cells were diluted by adding 150  $\mu$ L 1X-phosphate buffered saline (PBS). The numbers of ring-infected RBCs were counted using a Accuri C6 flow cytometer (BD biosciences). GraphPad Prism 5.0 software package (San Diego, CA) was used to calculate IC<sub>50</sub> using nonlinear regression.

### **Compound depletion assay**

His-tagged AMA1 protein (3D7 or FVO allele) or biotin-tagged RON2L peptide (500 pmol each) in 200  $\mu$ L were captured using dynabeads (Life technologies catalog # 10103D for His-tagged AMA1 capture or # 65601 for biotin-tagged RON2L peptide) for 1 hr at room temperature. Unbound protein or peptide was removed and beads were washed three times with 1x PBS. Next, the beads were incubated with 500 pmol of the inhibitor (NCGC00262650) in 200  $\mu$ L (10 $\mu$ M) and incubated for 1 hr at room temperature. The ability of AMA1 or RON2L peptide to bind the inhibitor was tested by capturing the beads on a magnet and collecting the supernatant. Inhibition of merozoite invasion by unbound inhibitor in the supernatants was performed as described above using purified, schizont-infected RBCs (FVO clone). Invasion efficiency was measured by counting the number of newly invaded rings by flow cytometry.

### **Transmission Electron Microscopy**

For ultrastructural analysis, merozoites in the presence of 2  $\mu$ M cytochalasinD were added to pre-warmed RBCs with or without 50  $\mu$ M AMA1-RON2 inhibitor (NCGC00262650 or NCGC00262654). Cells were fixed with 2.5% glutaraldehyde, 3% paraformaldehyde, 0.05 M phosphate buffer and 4% sucrose at room temperature for 2 hr and processed as described <sup>3</sup>.

### **Immunofluorescence Assay**

Mature schizonts were fixed with ice-cold acetone and blocked for 1 hr at room temperature (RT) in 1X phosphate buffered saline (PBS) containing 3% BSA and 0.1 % Triton X-100. Next, parasites were incubated with or without inhibitors in complete media for 1 hr at RT. Unbound inhibitor was removed and FITC-labeled RON2L peptide was added for 30 min at RT. Cells were washed in 1X PBS containing



0.1% Triton X-100. For microneme secretion analysis, mature schizonts were allowed to rupture in the presence or absence of the inhibitors. Released merozoites were fixed under non-permeabilizing conditions using 2.5% paraformaldehyde, 0.05% glutaraldehyde in 1X PBS for 10 min at RT. Microneme secretion was assessed by labeling merozoite with anti-AMA1 Pab and anti-rabbit Alexa 488 secondary antibody as described above. Images were captured using a Leica SP2 confocal microscope, processed using Huygens deconvolution software and visualized using Bitplane Imaris software.

### **Surface Plasmon Resonance (SPR) analysis**

SPR assay was performed using a BIAcore T100 instrument at 25<sup>0</sup>C according to manufacturer's recommendations. Recombinant AMA1 (100 µg/mL) was immobilized by amine coupling on a CM5 chip at a surface density of 7500 RU as described elsewhere<sup>43</sup>. For binding assay, each of the inhibitors were diluted in 10mM HEPES (pH 7.4), 150 mM NaCl, 0.05 % surfactant P20 and 3% DMSO (running buffer). As precipitation of the compounds was observed in the buffer used for SPR, samples were centrifuged and the supernatant containing soluble compound were used in the SPR assay.

Compounds were passed over the surface for 30 s at a flow rate of 30 microliter /min flow rate followed by a 100 s dissociation phase. Regeneration was done with a 15 s pulse of 10 mM glycine HCl (pH 2.5). The amount of inhibitor indicated in the figure is the concentration that was originally prepared as the actual concentration of the compounds present in the supernatant could not be measured.

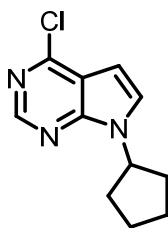
## Synthesis and spectral analysis of compounds NCGC00262650 and NCGC00262654

All air or moisture sensitive reactions were performed under positive pressure of nitrogen with oven-dried glassware. Anhydrous solvents such as dichloromethane, *N,N*-dimethylformamide (DMF), acetonitrile, methanol and triethylamine were purchased from Sigma-Aldrich. Preparative purification was performed on a Waters semi-preparative HPLC system. The column used was a Phenomenex Luna C18 (5 micron, 30 x 75 mm) at a flow rate of 45 mL/min. The mobile phase consisted of acetonitrile and water (each containing 0.1% trifluoroacetic acid). A gradient of 10% to 50% acetonitrile over 8 minutes was used during the purification. Fraction collection was triggered by UV detection (220 nm). Analytical analysis was performed on an Agilent LC/MS (Agilent Technologies, Santa Clara, CA).

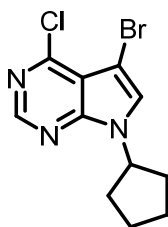
Method 1: A 7 minute gradient of 4% to 100% Acetonitrile (containing 0.025% trifluoroacetic acid) in water (containing 0.05% trifluoroacetic acid) was used with an 8 minute run time at a flow rate of 1 mL/min. A Phenomenex Luna C18 column (3 micron, 3 x 75 mm) was used at a temperature of 50 °C.

Method 2: A 3 minute gradient of 4% to 100% Acetonitrile (containing 0.025% trifluoroacetic acid) in water (containing 0.05% trifluoroacetic acid) was used with a 4.5 minute run time at a flow rate of 1 mL/min. A Phenomenex Gemini Phenyl column (3 micron, 3 x 100 mm) was used at a temperature of 50° C. Purity determination was performed using an Agilent Diode Array Detector for both Method 1 and Method 2. Mass determination was performed using an Agilent 6130 mass spectrometer with electrospray ionization in the positive mode. <sup>1</sup>H NMR spectra were recorded on Varian 400 MHz spectrometers. Chemical shifts are reported in ppm with undeuterated solvent (DMSO-d<sub>6</sub> at 2.49 ppm) as internal standard for DMSO-d<sub>6</sub> solutions. All of the analogs tested in the biological assays have purity greater than 95%, based on both analytical methods. High resolution mass spectrometry was recorded on Agilent 6210 Time-of-Flight LC/MS system. Confirmation of molecular formula was

accomplished using electrospray ionization in the positive mode with the Agilent Masshunter software (version B.02).

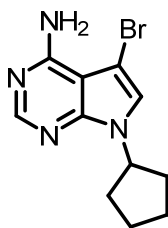


**4-Chloro-7-cyclopentyl-7H-pyrrolo[2,3-d]pyrimidine**<sup>44</sup>. NaH (95% w/w) (0.23 g, 9.77 mmol) was added to a solution of 4-chloro-7H-pyrrolo [2,3- d] pyrimidine (1.00 g, 6.51 mmol) in DMF (8 mL) at 0 °C. The resulting mixture was stirred at 0 °C for 30 min, and warmed to room temperature before the addition of bromocyclopentane (1.33 mL 12.4 mmol). The reaction was heated to 60 °C for 5 h, cooled to 0 °C and quenched with water. The aqueous layer was extracted with AcOEt (3x), and the combined organic layers were washed with water (1x), dried over Na<sub>2</sub>SO<sub>4</sub>, and concentrated. Purification by flash column chromatography (Hex/AcOEt acetate 9: 1) afforded the title compound as a clear glass-like oil. Yield 1.08 g, (75%). LC-MS: rt (min) 3.69 (short); (ESI): M<sup>+</sup>1=222.1/224.1.



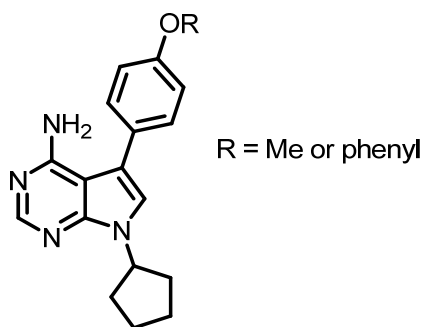
**5-bromo-4-chloro-7-cyclopentyl-7H-pyrrolo[2,3-d]pyrimidine**<sup>44</sup>: NBS (0.936 g, 5.26 mmol) was added to a stirred solution of 4-chloro-7-cyclopentyl-7H-pyrrolo[2,3-d]pyrimidine (1.08 g, 4.78 mmol) in CH<sub>2</sub>Cl<sub>2</sub> (14 mL). The reaction mixture was stirred for 18 h and the solvent was evaporated under reduced pressure to give a purplish solid. The resulting solid is washed with water and dried under

high vacuum to give the desired compound. Yield 1.22 g (85%) LC-MS: rt (min) 3.88 (short); (ESI):  $M^+1 = 300.0/302.0$ .



**5-bromo-7-cyclopentyl-7H-pyrrolo[2,3-d]pyrimidin-4-amine**<sup>44</sup>.

5-bromo-4-chloro-7-cyclopentyl-7H-pyrrolo[2,3-d]pyrimidine (1.2 g, 4.0 mmol), ammonium hydroxide (0.62 mL, 16.0 mmol), and 2M ammonia in MeOH (8 mL) were heated in a sealed tube at 100 °C for 48 h. The reaction mixture was concentrated under reduced pressure to a brown solid and triturated with diethyl ether to give 0.980 mg (87%) of the desired product. LC-MS: rt (min) 2.82 (short); (ESI):  $M^+1 = 281.0/283.0$ ; <sup>1</sup>H NMR (400 MHz, CD<sub>3</sub>OD)  $\delta$  1.50 - 1.95 (m, 6 H) 2.17 (d, 2 H) 4.98 - 5.14 (m, 1 H) 7.33 (s, 1 H) and 8.08 (s, 1 H).



**General procedure for Suzuki coupling**<sup>44</sup>

5-bromo-7-cyclopentyl-7H-pyrrolo[2,3-d]pyrimidin-4-amine (0.10 g, 0.36 mmol) was added to dioxane (10 mL) in a microwave vial under N<sub>2</sub>. 4M K<sub>2</sub>CO<sub>3</sub> (0.71 mL, 1.42 mmol), the requisite boronic acid (1.42 mmol), and bis(tri-*t*-butylphosphine)palladium(0) (2 mg, 0.004 mmol) were added and the resulting reaction mixture was heated in the microwave at 150 °C for 40 min. The reaction mixture was cooled

to room temperature, filtered through a pad of celite then siliamet DMT® resin loading 0.56 mmol/g was added to the solution and stirred at rt for 1 h. The resin was filtered, washed with dioxane, diluted with AcOEt (75 mL) and washed with saturated sodium bicarbonate (100 mL). The aqueous layer was extracted with AcOEt (1x) and the organic layers were combined, washed with brine, dried over Na<sub>2</sub>SO<sub>4</sub>, filtered and concentrated under reduced pressure. The compounds described below were purified using reversed-phase chromatography using a combiflash® system.

**7-cyclopentyl-5-(4-methoxyphenyl)-7H-pyrrolo[2,3-d]pyrimidin-4-amine.** The resulting crude brown solid was purified by reversed phase chromatography to give the desired product in 50% yield. LC-MS: rt (min) 2.08 (long); <sup>1</sup>H NMR (400 MHz, DMSO-*d*<sub>6</sub>) δ 1.57 - 1.75 (m, 2 H) 1.78 - 2.01 (m, 4 H) 2.03 - 2.23 (m, 2 H) 3.79 (s, 3 H) 5.03 - 5.19 (m, 1 H) 6.93 - 7.11(m, 2 H) 7.33 - 7.48 (m, 2 H) 7.63 (s, 1 H) and 8.39 (s, 1 H); <sup>13</sup>C NMR (100 MHz, DMSO-*d*<sub>6</sub>) δ 24.16, 32.75, 55.61, 55.98, 99.29, 115.09 , 118.37, 123.56, 123.65, 125.44, 130.20, 130.26, 147.95, 152.43, 159.21 and 159.39; HRMS (ESI) *m/z* (M+H)<sup>+</sup> calculated for C<sub>18</sub>H<sub>20</sub>N<sub>4</sub>O, 308.1640; found 308.1637.

**7-cyclopentyl-5-(4-phenoxyphenyl)-7H-pyrrolo[2,3-d]pyrimidin-4-amine**<sup>44</sup>. The brown oil was purified by reversed-phase chromatography to give the desired product in 47% yield. LC-MS: rt (min) 3.34 (long); <sup>1</sup>H NMR (400 MHz, CDCl<sub>3</sub>) δ 1.23 - 1.36 (m, 1 H) 1.75 - 1.98 (m, 7 H) 2.20 - 2.34 (m, 2 H) 5.18 - 5.29 (m, 1 H) 7.02 (s, 1 H) 7.04 - 7.12 (m, 4 H) 7.15 (t, *J* = 7.4 Hz, 1 H) 7.38 (t, *J* = 7.8 Hz, 2 H) 7.45 (d, *J* = 8.2 Hz, 2 H) and 8.33 (s, 1 H); HRMS (ESI) *m/z* (M+H)<sup>+</sup> calculated for C<sub>23</sub>H<sub>22</sub>N<sub>4</sub>O, 370.1795; found 370.1794.



## ***In Silico Modeling***

Crystal structures of AMA1 in the apo form (1Z40)<sup>21</sup> and RON2-bound complex (2Z8V)<sup>22</sup> were used to explore potential binding interactions of identified small molecule inhibitors to AMA1. A comparison of the apo AMA1 to the RON2-bound structure showed that the domain II loop (DII loop) is highly flexible (missing in the apo structure) and undergoes significant conformational changes upon RON2 peptide binding. Loops adjacent to the hydrophobic pocket (residues 172-176, 264-273 and 383-387) are disordered in the apo structure of AMA1. Whereas in the RON2-bound complex, AMA1 DII loop (residues 351-387) is displaced exposing the binding site for the N-terminal region of RON2 peptide.

The missing loops in the apo structure of AMA1 were re-modeled using MODELLER<sup>45</sup>. The resulting model of AMA1 was refined by energy minimization, followed by a 2-ns MD simulation in explicit solvent using the AMBER 12 package<sup>46</sup>. Five representative structures were extracted from the MD trajectory clustering analysis. The compounds were docked to the ensembles of AMA1 apo structure using the AutoDock 4.2<sup>47</sup>. The binding site was defined by an autogrid box so as to enclose the entire AMA1-RON2 binding interface along the hydrophobic groove for an extensive search for potential inhibitor binding site. A total of 50 poses were generated from each ensemble docking using the Lamarckian Genetic Algorithm (LGA). The maximum number of generations and energy evaluations were set to 27,000 and  $2 \times 10^6$ , respectively. All docked poses were clustered based on the root-mean square deviation (RMSD). The best binding models from top clusters were selected and further refined by a stepwise energy minimization and MD simulations.

The docking results of the small molecules with AMA1 showed two major “hotspot” regions that are favorable for inhibitor binding (Supplementary Figs. S7a and b). The first binding cluster is located near the flexible loop region, where a hydrophobic pocket is well-formed adjacent to DII loop (Figure S6a). In the first binding mode, compound NCGC00015280 and the two analogs NCGC00262650 and NCGC00262654 bound AMA1 in the pocket near the flexible DII loop region and forms extensive van der Waals and aromatic interactions with AMA1 residues F181, F183, Y251, F367. Because DII loop plays an important role in RON2 peptide binding<sup>22</sup>, a plausible mechanism is that these inhibitors bind the pocket and stabilize DII loop in a closed conformation, thereby, preventing RON2 from binding AMA1 (Supplementary Fig. S7a,e,g). The second binding mode is located at a more open and rigid region along the hydrophobic groove (Supplementary Fig. S7b,f,h), which is also important for RON2 peptide binding (interaction of RON2F2038 with AMA1F183 is needed for RON2 binding<sup>22</sup>). Other compounds in cluster 1 and the singletons (Supplementary Table S2) adopted binding modes similar to NCGC00015280 in the hydrophobic pocket and appeared to be well accommodated in the groove (Supplementary Figs. S7c and d).

## SUPPLEMENTARY REFERENCES

41. Baell, J. B. & Holloway, G. A. New substructure filters for removal of pan assay interference compounds (PAINS) from screening libraries and for their exclusion in bioassays. *J Med Chem* **53**, 2719-2740, (2010).
42. Smilkstein, M., Sriwilaijaroen, N., Kelly, J. X., Wilairat, P. & Riscoe, M. Simple and inexpensive fluorescence-based technique for high-throughput antimalarial drug screening. *Antimicrob Agents Chemother* **48**, 1803-1806 (2004).
43. Pal-Bhowmick, I. *et al.* Binding of aldolase and glyceraldehyde-3-phosphate dehydrogenase to the cytoplasmic tails of Plasmodium falciparum merozoite duffy binding-like and reticulocyte homology ligands. *MBio* **3**, [pii] 10.1128/mBio.00292-12 (2012).
44. Calderwood, D. J., Johnston, D. N., Munschauer, R. & Rafferty, P. Pyrrolo[2,3-d]pyrimidines containing diverse N-7 substituents as potent inhibitors of Lck. *Bioorg Med Chem Lett* **12**, 1683-1686, (2002).
45. Eswar, N. *et al.* Comparative protein structure modeling using Modeller. *Curr Protoc Bioinformatics* **Chapter 5**, Unit 5 6, (2006).
46. Case, D. A *et al.* AMBER 12, University of California, San Francisco, (2012).
47. Morris, G. M. *et al.* AutoDock4 and AutoDockTools4: Automated docking with selective receptor flexibility. *J Comput Chem* **30**, 2785-2791, (2009).